First Example of a Trimeric Metalloporphyrin. Synthesis, Electrochemical, and Spectroelectrochemical Studies of $[(P)Th(OH)_2]_3$ Where P Is the Dianion of Octaethyl- or Tetraphenylporphyrin. Crystal Structure of a Dihydrated Trinuclear Complex of Dihydroxy(5,10,15,20-tetraphenylporphinato)thorium(IV) Heptane Solvate

K. M. Kadish,*[1a] Y. H. Liu,[1a] J. E. Anderson,[1a] P. Charpin,[1b] G. Chevrier,[1b] M. Lance,[1b] M. Nierlich,[1b] D. Vigner,[1b] A. Dormond,[1c] B. Belkalem,[1c] and R. Guilard*[1c]

Contribution from the Department of Chemistry, University of Houston, Houston, Texas 77204-5641, Centre d'Etudes Nucleaires de Saclay, Laboratoire Associe au CNRS (UA331), 91191 Gif-sur Yvette Cedex, France, and Laboratoire de Synthese et d'Electrosynthese Organometallique, Associe au CNRS (UA 33), Faculte des Sciences "Gabriel", 21100 Dijon, France. *Received November 27, 1987*

Abstract: The reaction of $(P)ThCl_2$ with aqueous sodium carbonate in oxygen-free THF results in formation of dihydroxy complexes of the form $(P)Th(OH)_2$ where P is the dianion of octaethyl- or tetraphenylporphyrin. These complexes were characterized by mass spectral, IR, UV–visible, and NMR data. The crystal structure of $[(TPP)Th(OH)_2]_3 \cdot 2H_2O$ was determined by X-ray diffraction methods and gave the following crystallographic data: $[(TPP)Th(OH)_2]_3 \cdot 2H_2O \cdot 3C_7H_{16}$ or $[(C_{44}H_{28}N_4)_3Th_3(OH)_6 \cdot 2H_2O \cdot 3C_7H_{16}]$; MW 2973; rhombohedral; $R\bar{3}c$; $a = 17.962$ (9), $c = 73.75$ (2) Å; $V = 20605$ Å^3; $Z = 6$ (hexagonal cell); $D_{calcd} = 1.438$ g cm^{-3}; λ(Mo Kα) = 0.71073 Å; $F(000) = 7968$; $T = 295$ K; $R = 0.062$ for 754 independent reflections having $I \geq 2\sigma(I)$. The molecular unit is built around a threefold axis and the six OH^- ligands describe a trigonal prism. The triangular faces are capped by two H_2O molecules, while the three thorium atoms sit above the rectangular faces. The three TPP units lie parallel to the threefold axis, and each thorium metal is surrounded by a distorted square-archimedean antiprism. A heptane molecule is located between the TPP units, but atomic parameters were not determined for this species due to a very large disorder. The electrochemistry and spectroelectrochemistry of trimeric $[(TPP)Th(OH)_2]_3$ and $[(OEP)Th(OH)_2]_3$ were also investigated. Both complexes are oxidized and reduced at porphyrin ring based orbitals, and the potentials for $[(TPP)Th(OH)_2]_3$ are shifted by 360–510 mV relative to those of the $[(OEP)Th(OH)_2]_3$ complex. The trimeric complexes can be reversibly reduced in up to six one-electron-transfer steps depending upon the porphyrin macrocycle and the solvent. The complexes can also be oxidized by up to six electrons, which, for the case of $[(OEP)Th(OH)_2]_3$, occurs in a single three-electron-transfer process followed by three one-electron abstractions at more positive potentials. The initial three-electron oxidation of $[(OEP)Th(OH)_2]_3$ is reversible on the cyclic voltammetric time scale and gives theoretical values of $|E_{pa} - E_{pc}|$ and $|E_p - E_{p/2}|$ equal to 20 mV. These data are consistent with the simultaneous abstraction of one electron from each of the three $(OEP)Th(OH)_2$ units of $[(OEP)Th(OH)_2]_3$ and contrasts with both the oxidative behavior of $[(OEP)Th(OH)_2]_3^{3+}$ and the reductive behavior of $[(OEP)Th(OH)_2]_3$. Both of these complexes have interacting porphyrin units, which lead to reversible one-electron reductions separated by 170–210 mV and reversible one-electron oxidations separated by 50–100 mV in THF at −72 °C.

Prior to 1984, only one report of an actinide porphyrin complex had appeared in the literature.[2] The syntheses of dichloro and bis(acetylacetonato) complexes of the form $(P)MCl_2L_2$ and $(P)M(acac)_2$ where acac = acetylacetonate and M = Th or U have recently been reported,[3-6] and an X-ray crystal structure of $(TPP)UCl_2(THF)$ has been published.[5] The synthesized complexes are good starting products for the preparation of oxo or bis(μ-oxo) actinide porphyrins and are thus good models for the activation of molecular oxygen by coordination complexes.

The synthesis and structural properties of "triple-decker" porphyrins of the type $(P)_3M_2$ have recently been reported.[6] In the present paper we present the first synthesis, electrochemistry, solution characterization, and X-ray structure of a true trimeric metalloporphyrin. The investigated compounds are $[(P)Th(OH)_2]_3$ where P is the dianion of tetraphenylporphyrin (TPP) or octaethylporphyrin (OEP). These derivatives were synthesized by the reaction of $(P)MCl_2$ with sodium carbonate in oxygen-free THF. Characterization of the compounds was based on elemental analysis, ^{1}H NMR, IR, UV–visible, and mass spectral data. These data show that $[(P)Th(OH)_2]_3$ exists in different forms of aggregation depending upon the concentration of the porphyrin and the solvent. The compounds are trimeric at polarographic and ^{1}H NMR concentrations but dissociate into monomers as the concentration is decreased from $\sim 10^{-4}$ to $\sim 10^{-7}$ M in PhCN or THF. An X-ray crystal structure determination was also carried out for $[(TPP)Th(OH)_2]_3$, which is a hydrated trimer in the solid state. The present work thus provides the first examples of trimeric metalloporphyrins, which are characterized in both solution and the solid state.

Experimental Section

Chemicals. The synthesis of $(P)ThCl_2 \cdot 2C_6H_5CN$ was carried out under an argon atmosphere as previously reported.[4] All common solvents were thoroughly dried in an appropriate manner and were distilled under argon prior to use. All operations were carried out in Schlenk tubes under purified argon and with oxygen-free solvents. Reagent-grade tetrahydrofuran (THF) was distilled first from CaH_2 and then from sodium benzophenone under argon. Spectroscopic-grade methylene chloride (CH_2Cl_2) was purified by distillation over P_2O_5. Benzonitrile

(1) (a) University of Houston. (b) Centre d'Etudes Nucléaires de Saclay. (c) Université de Dijon.
(2) Wong, C.-P.; Horrocks, W. D. *Tetrahedron Lett.* **1975**, *31*, 2637.
(3) Dormond, A.; Belkalem, B.; Guilard, R. *Polyhedron* **1984**, *1*, 107.
(4) Dormond, A.; Belkalem, B.; Charpin, P.; Lance, M.; Vigner, D.; Folcher, G.; Guilard, R. *Inorg. Chem.* **1986**, *25*, 4785.
(5) Girolami, G. S.; Milam, S. N.; Suslick, K. S. *Inorg. Chem.* **1987**, *26*, 343.
(6) Buchler, J. W.; Cian, A. D.; Fischer, J.; Kihn-Botulinski, M.; Paulus, H.; Weiss, R. *J. Am. Chem. Soc.* **1986**, *108*, 3652.

0002-7863/88/1510-6455$01.50/0

(PhCN) was distilled over P_2O_5 under reduced pressure. Tetra-*n*-butylammonium perchlorate (TBAP) was purchased from Fluka Chemical Corp., purified by two recrystallizations from ethyl alcohol, and stored in a vacuum oven at 40 °C.

Preparation of [(TPP)Th(OH)$_2$]$_2$. A total of 0.44 mmol of (TPP)$ThCl_2 \cdot 2C_6H_5CN$ in 30 mL of tetrahydrofuran was added to 150 mL of an oxygen-free 10% solution of sodium carbonate at room temperature. The reaction was monitored by UV–visible spectroscopy. After the reaction was completed, the solution was filtered and the brown-purple precipitate dried and extracted with 40 mL of THF. The resulting THF solution was concentrated to 15 mL without heating after which 10 mL of heptane was added. The solution was then cooled to −20 °C and filtered to give 0.28 g (80%) of purple crystals. Anal. Calcd for $C_{44}H_{30}N_4O_2Th \cdot 0.66H_2O \cdot C_7H_{16}$: C, 62.17; H, 4.78; N, 5.54; Th, 23.74. Found: C, 61.82; H, 4.03; N, 5.65; Th, 23.43.

Preparation of [(OEP)Th(OH)$_2$]$_2$. A total of 0.48 mmol of (OEP)$ThCl_2 \cdot 2C_6H_5CN$ in THF was reacted with sodium carbonate as described for $(TPP)Th(OH)_2$. The THF was evaporated to give a purple precipitate, which was dried and extracted three times with 20 mL of pentane. The pentane solution was then concentrated to 5 mL and cooled to −70 °C to give 0.314 g (82%) of red crystals, which were very soluble in pentane. Anal. Calcd for $C_{36}H_{46}N_4O_2Th \cdot 0.66H_2O \cdot C_5H_{12}$: C, 54,49; H, 6.36; N, 6.03; Th, 26.22. Found: C, 55.78; H, 6.69; N, 6.35; Th, 26.30.

Physicochemical Measurements. Elemental analyses were performed by the Service de Microanalyses du CNRS. Mass spectra were recorded in the electron-impact mode with a Finnigan 3300 spectrometer (ionization energy 30–70 eV, ionization current 0.4 mA, source temperature 250–400 °C). ^1H NMR spectra were recorded at 400 MHz on a Bruker WM 400 spectrometer of the Cerema (Centre de Resonance Magnetique of the University of Dijon). Spectra were measured from 5 mg solutions of the complex in $CDCl_3$ with tetramethylsilane as internal reference. Infrared spectra were prepared as either a 1% dispersion in CsI pellets or in THF. Electronic absorption spectra were recorded on either a Perkin-Elmer 559 spectrophotometer or an IBM Model 9430 spectrophotometer.

Cyclic voltammetric measurements were obtained with either an IBM EC 225 voltammetric analyzer or an EG&G Princeton Applied Research Model 174A/175 polarographic analyzer/potentiostat. This latter instrument was coupled with an EG&G Model 9002A X-Y recorder for potential scan rates less than 500 mV/s or a Tektronix Model 5111 storage oscilloscope for scan rates equal to or larger than 500 mV/s. Thin-layer spectroelectrochemical measurements were made with an IBM EC 225 voltammetric analyzer coupled with a Tracor Northern 1710 spectrometer/multichannel analyzer.

Platinum working and counter electrodes were used for all electrochemical measurements, which were performed under an inert atmosphere by Schlenk techniques. The thin-layer spectroelectrochemical cell has been previously described.[7] A saturated calomel electrode (SCE) was separated from the bulk of the solution by a fritted-glass disk junction and was used as the reference electrode. The ferrocene/ferrocenium (Fc/Fc^+) couple was also used as an internal reference standard for potential measurements. The supporting electrolyte for electrochemical studies was tetrabutylammonium perchlorate (TBAP).

Determination of Crystal and Molecular Structure and Crystal Data. The data were collected on an Enraf-Nonius CAD-4 diffractometer. The cell dimensions were refined by a least-squares fitting of θ values of 25 reflections in the range 8–12°. A total of 3401 reflections was collected in one-fourth of the reciprocal sphere to obtain more significant intensity measurements from a tiny crystal.

A total of 754 unique reflections with $I \geq 2\sigma(I)$ were considered as observed. Lorentz and polarization corrections were applied. Three standard reflections, monitored every 1 h, gave the intensity decay (−0.11%/h, −6.4% total), which was taken into account. The data were corrected for absorption with the program DIFABS[19] with minimum and maximum transmission factors of 0.6292 and 1.2432, respectively.

Crystal data and other details on the crystal structure refinement are given in Table I. Only the Th atom was given anisotropic thermal parameters. Hydrogen atoms were introduced in ideal positions and then constrained to ride their carbon atoms (C–H, 0.95 Å). Atomic coordinates and temperature factors are given in Table II. Solvent molecules were detected in the last difference Fourier among peaks no higher than 0.3–0.4 e/Å^3, indicating severe disorder.

Results and Discussion

The syntheses of $[(TPP)Th(OH)_2]_2$ and $[(OEP)Th(OH)_2]_2$ were accomplished in 80–82% yield as described in the Experimental Section. Elemental analyses and mass spectral data of the complexes (Table III) demonstrate the presence of both solvent and water molecules in the solid. The molecular peak $[(P)Th(OH)_2]^+$ is observed for both complexes. There are also $[M + 1]^+$ and $[M + 2]^+$ peaks, which can be attributed to the fragments $[(P)Th(OH)(H_2O)]^+$ and $[(P)Th(H_2O)_2]^+$. An intense peak corresponding to $[(P)Th(H_2O)]^+$ is also observed in the mass spectrum. The presence of these ions provides good evidence for water molecules coordinated to the central Th(IV) metal. However, they could also result from a recombination of $(P)Th(OH)_2$ with one or two hydrogen atoms. The presence of a

Table I. Crystal Data and Structure Analysis

formula	$C_{132}H_{94}N_{12}O_8Th_3 \cdot 3C_7H_{16}$
MW	2973
cryst solvent	THF/heptane 1.5/1.0
cryst color, habit, dimens, mm	red violet, prismatic, 0.16 × 0.14 × 0.08
cryst syst, space gp	rhombohedral, $R\bar{3}c$
lattice param (hexagonal axis)	
a, Å	17.962 (9)
c, Å	73.75 (2)
V, Å^3; Z	20 605; 6
D_{calcd}, g cm^{-3}	1.438
$F(000)$	8868
radiatn	Mo Kα (d = 0.710 73 Å) graphite monochromator
temp, K	295
μ(Mo Kα), cm^{-1}	34.11
range, deg	1–18
octants	$\pm h, +k, +l$ (−15 + 15, 0 + 15, 0 + 64)
no. of unique data with $I \geq 2\sigma(I)$	754
no. of param	106
scattering factors (f', f'') sources	ref 20
structure soln	heavy-atom method
$R(F)$	0.061
$R_w(F)$	0.081
w (weights)	$4F_o^2/[(\sigma(I))^2 - (pF_o^2)^2]$ with p = 0.06
computer programs	Frenz, B. A. *Enraf-Nonius Structure Determination Package—SDP Users Guide Version*, Jan 6, 1983

Table II. Atomic Coordinates and Isotropic or Equivalent Temperature Factors with Their Estimated Standard Deviations

atom	x	y	z	B, Å^2
Th[a]	0.1273 (3)	0.1273	0.250	2.48 (4)
O(1)	−0.001 (1)	0.095 (1)	0.2679 (3)	2.7 (6)
O(2)	0.000	0.000	0.3019 (8)	12 (2)
N(1)	0.273 (2)	0.145 (2)	0.2555 (3)	3.4 (8)
N(2)	0.194 (2)	0.217 (2)	0.2783 (4)	3.2 (7)
C(1)	0.325 (2)	0.138 (2)	0.2433 (4)	4 (1)
C(2)	0.387 (2)	0.124 (3)	0.2516 (5)	5 (1)
C(3)	0.366 (2)	0.115 (2)	0.2694 (5)	5 (1)
C(4)	0.300 (2)	0.138 (2)	0.2733 (4)	2.7 (9)
C(5)	0.228 (2)	0.182 (2)	0.2914 (5)	4 (1)
C(6)	0.215 (2)	0.223 (2)	0.3068 (5)	5 (1)
C(7)	0.178 (2)	0.271 (2)	0.3055 (5)	6 (1)
C(8)	0.170 (2)	0.275 (2)	0.2864 (5)	5 (1)
C(9)	0.270 (2)	0.146 (2)	0.2880 (4)	2.7 (9)
C(10)	0.304 (2)	0.126 (2)	0.3055 (2)	5 (1)
C(11)	0.385 (2)	0.171 (2)	0.3124 (5)	6 (1)
C(12)	0.412 (3)	0.148 (3)	0.3274 (6)	9 (2)
C(13)	0.353 (3)	0.080 (2)	0.3355 (6)	8 (1)
C(14)	0.268 (3)	0.025 (3)	0.3323 (6)	8 (1)
C(15)	0.242 (2)	0.050 (2)	0.3148 (5)	6 (1)
C(16)	0.328 (2)	0.147 (2)	0.2245 (4)	4 (1)
C(17)	0.393 (2)	0.145 (2)	0.2134 (5)	6 (1)
C(18)	0.481 (3)	0.211 (4)	0.2135 (7)	15.0
C(19)	0.536 (3)	0.225 (3)	0.1966 (7)	15.0
C(20)	0.523 (3)	0.143 (3)	0.1941 (7)	11 (2)
C(21)	0.452 (3)	0.076 (3)	0.1968 (5)	8 (1)
C(22)	0.391 (3)	0.079 (3)	0.2059 (6)	9 (2)

[a] Th atom was refined anisotropically: $B_{eq} = {}^4/_3[a^2\beta_{11} + b^2\beta_{22} + c^2\beta_{33} - {}^1/_2ab(\cos\gamma)\beta_{12}]$.

(7) Lin, X.-Q.; Kadish, K. M. *Anal. Chem.* **1985**, *57*, 1498.

Table III. Mass Spectral Data for $[(P)Th(OH_2)_2]_3$

fragment	$[(OEP)Th(OH)_2]_3$ m/e	rel intens, %	$[(TPP)Th(OH)_2]_3$ m/e	rel intens, %
$[(P)Th(OH_2)_2]^+$	800	100	880	78
$[(P)Th(OH)(OH_2)]^+$	799	46	879	100
$[(P)Th(OH)_2]^+$	798	34	878	76
$[(P)Th(OH_2)]^+$	782	51	862	23
$[(P)Th(OH)]^+$	781	83	861	40
$[(P)ThO]^+$	780	65	860	27

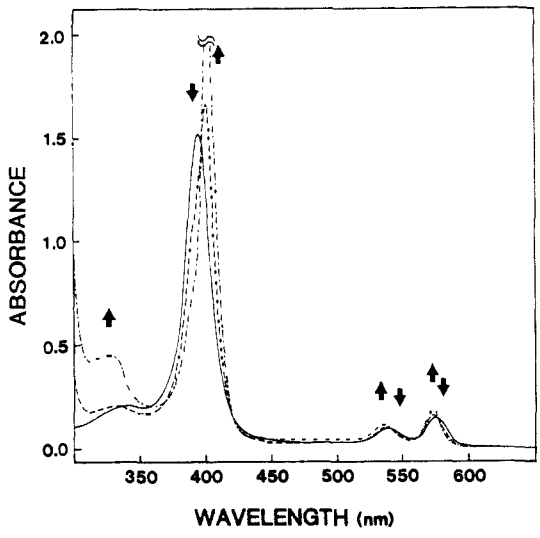

Figure 1. UV-visible spectra of $[(OEP)Th(OH)_2]_3$ in PhCN containing 0.2 M TBAP at a concentration of 2.7×10^{-4} M (—), 2.7×10^{-6} M (---), and 5.4×10^{-7} M (-·-).

peak for $[(P)ThO]^+$ suggests the loss of one water molecule from the dihydroxo $(P)Th(OH)_2$ unit.

Infrared data for the $[(P)Th(OH)_2]_3$ complexes confirm the presence of OH^- groups coordinated to the thorium metal. The O–H stretching modes of the ligand are located at 3580 cm^{-1}. Two bands are found at 430 and 350 cm^{-1} and can be attributed to the Th–O and Th–N stretching modes, respectively.

A summary of NMR data for $[(TPP)Th(OH)_2]_3$ and $[(OEP)Th(OH)_2]_3$ is given in Table IV. Both complexes exhibit ^1H NMR features typical of diamagnetic metalloporphyrins. The meso protons of $[(OEP)Th(OH)_2]_3$ are located at 9.94 ppm whereas the methylic protons give a triplet at 1.77 ppm. Two multiplets are clearly observed at 4.50 and 4.18 ppm for the methylenic protons, and this results from an ABX_3 coupling with the methylic protons.[8,9] The difference between the resonance frequencies of the methylenic protons, $|\delta_A - \delta_B|$, indicates that the axial ligands induce a large inequivalence between the two porphyrin faces. This can be due to an out-of-plane displacement of the metal atom or a cis coordination of the two axial ligands.

A broad peak is located at −4.36 ppm for $[(OEP)Th(OH)_2]_3$ and is due to the OH^- anion. This peak disappears after addition of D_2O and is not observed if the solid sample is dried at temperatures higher than 30 °C. This observation is typical for cases of molecular association. The bound OH^- anion of $[(TPP)Th(OH)_2]_3$ has a signal at −3.88 ppm and has the same characteristics as the hydroxide anion of $[(OEP)Th(OH)_2]_3$. The pyrrole protons of $[(TPP)Th(OH)_2]_3$ appear as a singlet at 8.55 ppm.

More structural information is given by the chemical shifts of the phenyl protons on $[(TPP)Th(OH)_2]_3$. The ortho protons of $[(TPP)Th(OH)_2]_3$ are not equivalent and give two multiplets at 8.22 and 7.60 ppm. This lack of equivalence results from an asymmetry with respect to the porphyrin plane.[10,11] The ^1H NMR

Figure 2. Stereoview of the trimeric unit (Johson, C. K. ORTEP; Report ORNL 3794; Oak Ridge National Laboratory: Oak Ridge, TN, 1965).

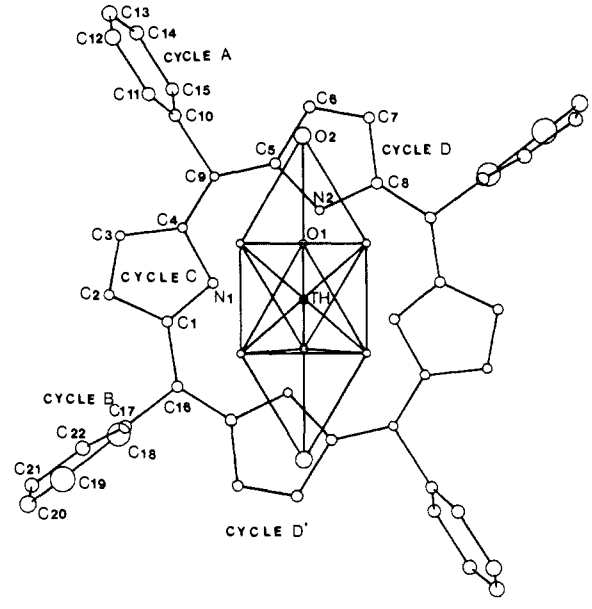

Figure 3. Labeling of atoms in the asymmetrical unit.

characteristics of $[(TPP)Th(OH)_2]_3$ confirm the nonequivalence of the two porphyrin faces and suggest a cis coordination of the two axial ligands. The meta and para protons have resonances at 7.86 and 7.23 ppm, respectively. Signals attributed to the solvent of recrystallization are also clearly observed, even when the sample is dried under vacuum.

Electronic absorption spectra of $[(TPP)Th(OH)_2]_3$ and $[(OEP)Th(OH)_2]_3$ belong to the normal class.[12] UV-visible data of $[(OEP)Th(OH)_2]_3$ and $[(TPP)Th(OH)_2]_3$ at various concentrations in PhCN and THF containing 0.2 M TBAP are reported in Table V while Figure 1 shows the UV-visible spectra of $[(OEP)Th(OH)_2]_3$ at concentrations between 2.7×10^{-4} and 5.4×10^{-7} M in benzonitrile.

The spectrum of 2.7×10^{-4} M $[(OEP)Th(OH)_2]_3$ has a Soret band at 396 nm and two visible bands at 539 and 575 nm. The Soret band shifts to 403 nm and a new band appears at 328 nm as the porphyrin concentration is decreased to 5.4×10^{-7} M. All of the spectra pass through isosbestic points at 398, 540, and 577 nm, indicating the presence of only two spectroscopically observable species in equilibrium. Likewise, the three bands of $[(TPP)Th(OH)_2]_3$ at 414, 552, and 587 nm shift to 430, 560, and 602 nm upon decreasing the porphyrin concentration from 1.03×10^{-4} to 2.05×10^{-7} M. At the same time, a new band grows in at 332 nm. These spectra do not pass through a single isosbestic point as is the case for $[(OEP)Th(OH)_2]_3$ and thus indicate several different forms of the complex in dilute solutions.

The concentration dependence of the $[(OEP)Th(OH)_2]_3$ and $[(TPP)Th(OH)_2]_3$ spectra in Figure 1 and Table V clearly demonstrates that two or more forms of the complex can exist in PhCN or THF. The changes in spectra for $[(OEP)Th(OH)_2]_3$ suggest a trimer–monomer equilibrium while, for the case of $[(TPP)Th(OH)_2]_3$, a trimer–dimer–monomer series of equilibria is postulated to occur.

(8) Scheer, H.; Katz, J. J. In *Porphyrins and Metalloporphyrins*; Smith, K. M., Ed.; Elsevier: Amsterdam, The Netherlands, 1975; Chapter 10, and references therein.
(9) Busby, C. A.; Dolphin, D. *J. Magn. Reson.* **1976**, *23*, 211.
(10) Abraham, R. J.; Smith, K. M. *Tetrahedron Lett.* **1971**, *36*, 3335.
(11) Janson, T. R.; Katz, J. J. In *The Porphyrins*; Dolphin, D., Ed.; Academic: New York, 1978; Vol. IV, Chapter 1, and references therein.
(12) Gouterman, M. In *The Porphyrins*; Dolphin, D., Ed.; Academic: New York, 1978; Vol. III, Chapter 1, and references therein.

Table IV. ^{1}H NMR Data for [(P)Th(OH)$_2$]$_3$

porphyrin (P)	R^1	R^2	protons of R^1			protons of R^2			bound OH$^-$		solvent[b]	
				mult/i[a]	δ		mult/i	δ	mult/i	δ	mult/i	δ
OEP	H	C_2H_5		s/4	9.94	CH_2	m/8	4.50	s/2	−4.36[c]	m[d]	1.33
							m/8	4.18			m[d]	0.97
						CH_3	t/24	1.77				
TPP	C_6H_5	H	*o*-H	m/4	8.22		s/8	8.55	s/2	−3.88[c]	m/10	1.35
			o'-H	m/4	7.60						m/6	0.99
			m-H	m/8	7.86							
			p-H	m/4	7.23							

[a] Key: mult = multiplicity, i = number of protons, s = singlet, t = triplet, m = multiplet. [b] C_5H_{12} for [(OEP)Th(OH)$_2$]$_3$ and C_7H_{16} for [(TPP)Th(OH)$_2$]$_3$. [c] Very broad signal disappears after addition of D_2O. [d] Intensity of peak depends upon sample drying time.

Table V. Concentration Dependence of [(OEP)Th(OH)$_2$]$_3$ and [(TPP)Th(OH)$_2$]$_3$ UV-Visible Spectra in PhCN and THF Containing 0.2 M TBAP

compd	solvent	concn, M	λ_{max}, nm (apparent[a] molar absorptivity ($\epsilon \times 10^{-4}$), M^{-1} cm^{-1})			
[(OEP)Th(OH)$_2$]$_3$	PhCN	2.7×10^{-4}		396 (56.3)	539 (3.3)	575 (5.1)
		2.7×10^{-6}		402 (61.4)	538 (3.5)	574 (5.7)
		5.4×10^{-7}	328 (16.9)	403 (82.1)	536 (4.3)	573 (7.0)
[(TPP)Th(OH)$_2$]$_3$	THF	1.03×10^{-4}		414 (102.1)	552 (6.2)	587 (1.0)
		1.03×10^{-6}	332 (36.5)	425 (103.7)	556 (6.3)	596 (1.5)
		2.05×10^{-7}	332 (99.5)	430 (115.4)	560 (6.8)	602 (2.9)

[a] Spectra at low concentrations correspond to a mixture of monomers and trimers for the case of [(OEP)Th(OH)$_2$]$_3$ and to monomers, dimers, and trimers for the case of [(TPP)Th(OH)$_2$]$_3$.

Table VI. Bond Distances (Å) of [(TPP)Th(OH)$_2$]$_3$ with Their Esd's

Th–Th	3.960 (3)	C(1)–C(2)	1.39 (4)
Th–O(1)	2.46 (2)	C(1)–C(16)	1.40 (3)
Th–N(1)	2.50 (2)	C(2)–C(3)	1.36 (3)
Th–N(2)	2.54 (2)	C(3)–C(4)	1.47 (3)
N(1)–N(2)	2.87 (3)	C(4)–C(9)	1.25 (4)
N(1)–C(1)	1.36 (4)	C(5)–C(6)	1.44 (4)
N(1)–C(4)	1.43 (3)	C(5)–C(9)	1.24 (4)
N(2)–C(5)	1.44 (3)	C(6)–C(7)	1.33 (4)
N(2)–C(8)	1.45 (3)	C(7)–C(8)	1.43 (4)
		C(9)–C(10)	1.55 (4)
		C(16)–C(17)	1.45 (4)

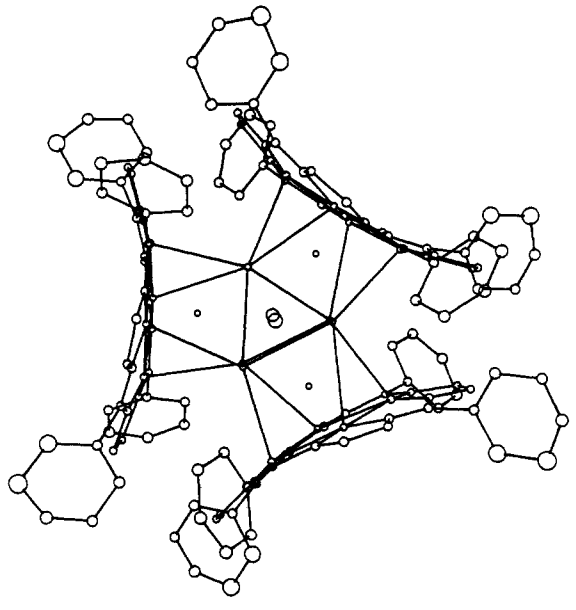

Figure 4. Projection of the trimeric unit along the *c* axis.

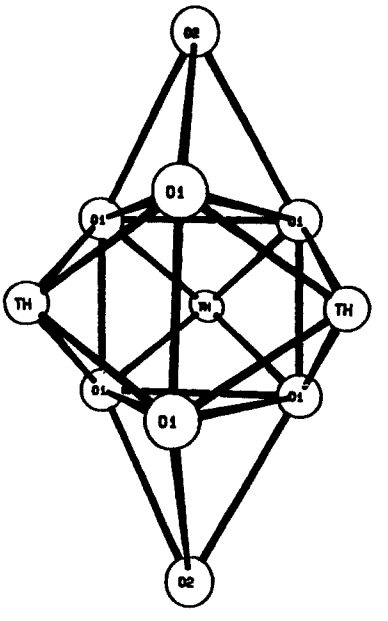

Figure 5. ORTEP drawing of the $Th_3(OH)_6(OH_2)_2$ core.

Table VII. Bond Angles (deg) of [(TPP)Th(OH)$_2$]$_3$ with Their Esd's

O(1)–Th–N(1)	137.7 (6)	N(1)–C(4)–C(9)	127 (3)
O(1)–Th–N(2)	78.5 (6)	C(3)–C(4)–C(9)	131 (4)
N(1)–Th–N(2)	69.6 (8)	N(2)–C(5)–C(6)	96 (3)
Th–N(1)–N(2)	55.9 (6)	N(2)–C(5)–C(9)	126 (4)
Th–N(2)–N(1)	54.9 (6)	C(6)–C(5)–C(9)	136 (3)
C(1)–N(1)–C(4)	108 (2)	C(5)–C(6)–C(7)	122 (3)
C(5)–N(2)–C(8)	112 (3)	C(6)–C(7)–C(8)	102 (3)
N(1)–C(1)–C(2)	113 (3)	N(2)–C(8)–C(7)	107 (3)
N(1)–C(1)–C(16)	129 (3)	C(4)–C(9)–C(5)	130 (3)
C(2)–C(1)–C(16)	119 (3)	C(4)–C(9)–C(10)	117 (4)
C(1)–C(2)–C(3)	104 (3)	C(5)–C(9)–C(10)	112 (3)
C(2)–C(3)–C(4)	112 (4)	C(1)–C(16)–C(17)	122 (3)
N(1)–C(4)–C(3)	102 (3)		

An X-ray crystallographic study demonstrates that [(TPP)-Th(OH)$_2$]$_3$ is trimeric in the solid state. Figure 2 represents the stereoview of [(TPP)Th(OH)$_2$]$_3$·2H$_2$O while Figure 3 gives the atomic labeling for one macrocycle around the trigonal prism defined by the OH$^-$ anions. Figure 4 shows the projection of a molecular unit on the (001) plane, and Figure 5 shows the ORTEP drawing of the $Th_3(OH)_6(OH_2)_2$ core. The atomic coordinates and isotropic or equivalent temperature factors are given in Table II, and a full listing of the crystallographic parameters is given as supplementary material.

The characteristic distances and angles of the [(TPP)Th(OH)$_2$]$_3$ trimer are given in Tables VI and VII. There are six units containing three thorium atoms in the nonprimitive hexagonal cell. Each trimer is situated about a 32 site (6a). The six OH$^-$ ions

Table VIII. Oxidation and Reduction Potentials (V vs SCE) of $[(OEP)Th(OH)_2]_3$ and $[(TPP)Th(OH)_2]_3$ in Nonaqueous Media, Containing 0.2 M TBAP

compd	solvent	temp, °C	reduction processes[a]						oxidation processes[a]					
			1	2	3	4	5	6	7	8	9	10	11	12
$[(OEP)Th(OH)_2]_3$	THF	23	−1.51	−1.67	−1.87[b]				0.69				0.80	0.96
		−72	−1.49	−1.70	−1.87				0.66	0.99	1.04	1.14		
	CH_2Cl_2	23	−1.65	−1.86					0.61	1.08[b]	1.22[b]	1.34[b]	0.61	0.85
		−70	−1.64	−1.85	−2.03				0.61	1.03	1.19[c]	1.19[c]		
	PhCN	23	−1.62	−1.81					0.62	1.00[b]	1.15[b]	1.28[b]	0.68	0.83
		−9	−1.62	−1.82					0.63	0.97	1.13	1.26		
$[(TPP)Th(OH)_2]_3$	THF	23	−1.12	−1.24	−1.37	−1.62[b]	−1.78[b]	−1.93[b]	1.05[b]					
		−55	−1.13	−1.27	−1.36	−1.76[b]	−2.00[b]	−2.10[b]	1.08[b]					

[a] Processes 1–12 are defined by the peaks in the voltammograms illustrated in Figures 5, 7, and 9. [b] Values of peak potential, E_p, at a scan rate of 0.10 V/s. [c] Processes 9 and 10 are overlapped to form a single two-electron-transfer wave.

[O(1)] define a trigonal prism capped by two water molecules [O(2)] on its triangular faces and three thorium atoms on its rectangular faces along the three horizontal twofold axes. Moreover, the three tetraphenylporphyrin units are parallel to the threefold axis, leading to an almost regular archimedean antiprism surrounding each thorium atom. This square antiprism consists of four bridging OH^- ions and the four nitrogen atoms of TPP. The Th–N(1) bond distance of 2.50 (2) Å and the Th–N(2) bond distance of 2.54 (2) Å are statistically equal and somewhat larger than the Th–O(1) bond distance of 2.46 (2) Å. The Th–Th distance is 3.960 (3) Å and does not suggest any metal–metal interaction.

The conformation of the porphyrin chain is comparable to that already described for $(OEP)Th(acac)_2$.[4] It shows a convexity directed to the heavy atom. The phenyl cycle consisting of C(10)–C(11)–C(12)–C(13)–C(14)–C(15) (cycle A) is rigorously planar and has the largest deviations, which are less than ±0.03 (5) Å. In the other phenyl cycle consisting of C(17)–C(18)–C(19)–C(20)–C(21)–C(22) (cycle B), the largest deviation from the mean plane is less than or equal to ±0.22 (7) Å. This distortion concerns carbon atoms C(18) and C(19), which are affected with large isotropic thermal factors (and have been fixed at 15 $Å^2$ in the refinement). The position of C(19), close to a threefold axis, implies the vicinity of two other C(19) atoms, which belong to other trimeric species and may generate some disorder related to steric hindrance. The pyrrolic cycles N(1)–C(1)–C(2)–C(3)–C(4) (cycle C) and N(2)–C(5)–C(6)–C(7)–C(8) (cycle D) are also planar; the largest deviations from the mean plane are ≤0.05 (4) and <0.04 (4) Å, respectively.

If the base plane of the porphyrin is defined by the four N atoms, the angles with pyrrole cycles C and D are 19.5° and 9.8°, respectively. This is in agreement with the convexity of the porphyrin macrocycle. The phenyl cycles A and B are approximately perpendicular (91°) to each other as they are with the porphyrin base plane (80° and 81.4°).

The heptane molecules found in the ^1H NMR spectra were detected at the end of the crystal structure determination on the last Fourier difference synthesis and are located between trimeric units and centered on the twofold axes ($x = 0.589$, $y = 0$, $z = {}^1/_4$). All attempts to refine the heptane with a single set of atomic positions failed, which indicates a high degree of static or dynamic disorder.

Reduction of $[(OEP)Th(OH)_2]_3$. A cyclic voltammogram of 1.4×10^{-3} M $[(OEP)Th(OH)_2]_3$ in THF at −72 °C is shown in Figure 6a. The compound exists as the associated trimer at this polarographic concentration and undergoes three reversible, one-electron-reduction processes. These reductions are labeled as processes 1–3 and occur at $E_{1/2} = -1.49$, −1.70, and −1.87 V vs SCE. A similar cyclic voltammogram was obtained in CH_2Cl_2 at −70 °C.

The first two reductions of trimeric $[(OEP)Th(OH)_2]_3$ remain reversible at room temperature on the cyclic voltammetric time scale, but this is not the case for the third reduction. At a scan rate of 0.10 V/s, processes 1 and 2 occur at $E_{1/2} = -1.51$ and −1.67 V while process 3 is located at $E_p = -1.87$ V. Processes 1 and 2 have an $|E_{pa} - E_{pc}| = 60$ mV, an $|E_p - E_{p/2}| = 60$ mV, and a constant value of $i_p/v^{1/2}$, thus indicating diffusion-controlled

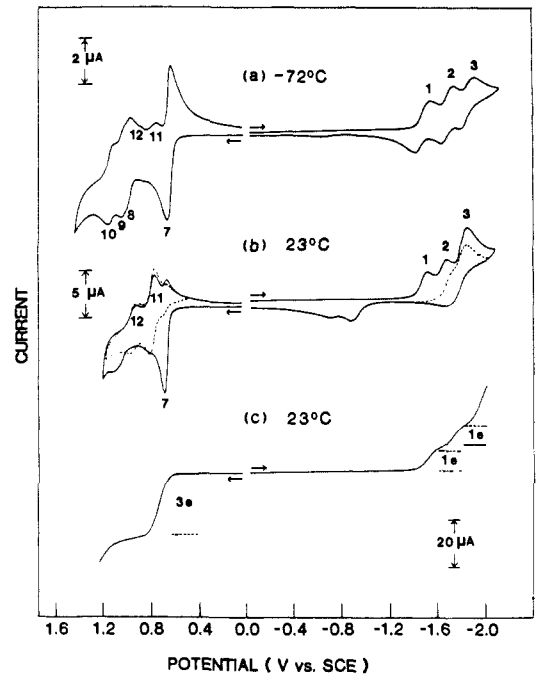

Figure 6. Cyclic voltammograms (scan rate 0.10 V/s) of 1.4×10^{-3} M $[(OEP)Th(OH)_2]_3$ in THF, 0.2 M TBAP, (a) at −72 °C and (b) at 23 °C during first scan (—) and second scan (- - -) and (c) rotating-disk voltammogram of 1.4×10^{-3} M $[(OEP)Th(OH)_2]_3$ in THF, 0.2 M TBAP. Rotation rate 900 rpm.

one-electron transfers. The peak for process 3 also has an $|E_p - E_{p/2}| = 60$ mV but has no return oxidation peaks coupled to the reduction. Reoxidation peaks are also not coupled to the first two reductions if the potential is scanned past potentials for the third reduction at a scan rate of 0.10 V/s. This suggests a dissociation of the triply reduced trimer and is shown in Figure 6b. A dissociation of the complex is not observed to occur at higher scan rates. Under these conditions, the third reduction becomes more reversible and the voltammograms are similar to those obtained at low temperature. Almost identical electrochemical behavior is found for the reduction of $[(OEP)Th(OH)_2]_3$ in THF, CH_2Cl_2, and PhCN, and reduction potentials in these three solvents are listed in Table VIII.

Analysis of the cyclic voltammetric curves demonstrates that the third reduction of $[(OEP)Th(OH)_2]_3$ involves a one-electron transfer followed by a fast chemical reaction and an additional one or more electron reduction (an electrochemical ECE type mechanism). Increased values of $i_p/v^{1/2}$ are obtained for this process at low scan rates, which indicate that a further reduction occurs after the chemical reaction. The product of the chemical reaction is unknown but is characterized by reoxidation peaks at $E_p = -1.69$, −0.87, and −0.70 V when the potential scan rate is 0.10 V/s.

The site of electron transfer for the first two reductions of $[(OEP)Th(OH)_2]_3$ is at the porphyrin π ring system, and this was demonstrated by both ESR and UV–visible spectral monitoring

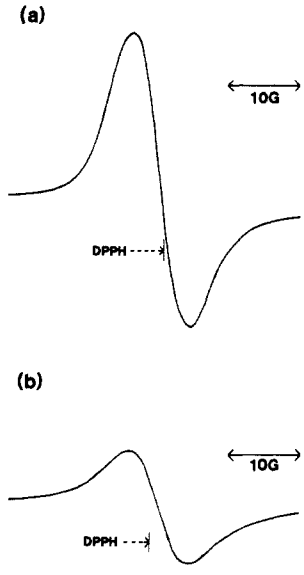

Figure 7. ESR spectra of (a) $[(OEP)Th(OH)_2]_3$ after electrolysis at −1.60 V for 3 min and (b) $[(TPP)Th(OH)_2]_3$ after electrolysis at −1.19 V for 3 min. Both spectra were measured at 133 K in THF containing 0.2 M TBAP.

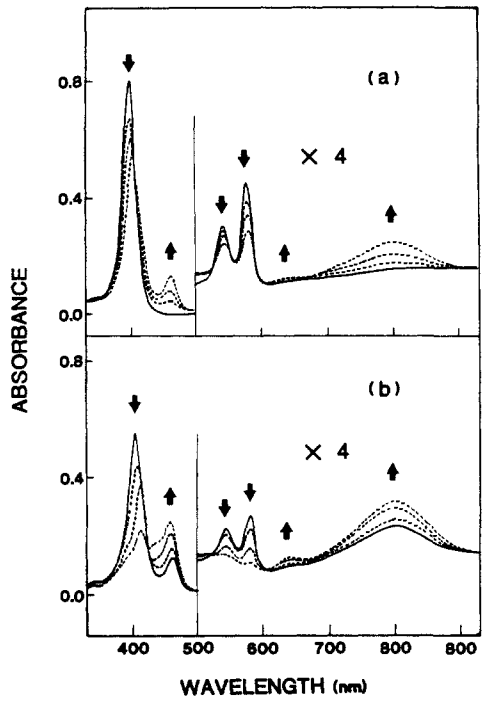

Figure 8. UV–visible spectra of $[(OEP)Th(OH)_2]_3$ in PhCN, 0.2 M TBAP, upon stepping the potential (a) from 0.00 to −1.70 V and (b) from −1.70 to −1.95 V.

of the electroreduced product. The ESR spectrum of $[(OEP)Th(OH)_2]_3^-$ with a g value of 2.003 is shown in Figure 7a and is clearly characteristic of a porphyrin π anion radical. The UV–visible spectrum of singly reduced $[(OEP)Th(OH)_2]_3$ is also characteristic of a porphyrin π anion radical. The original complex is characterized by electronic absorption bands at 396, 539, and 575 nm. These bands decrease in intensity during both reductions and bands typical of a metalloporphyrin π anion radical[13] appear at 411, 456, and 799 nm. This is shown in parts a and b of Figure 8. The molar absorptivity of the band at 456 nm increases from 9.3×10^4 to 18.1×10^4 M^{-1} cm^{-1} upon going from $[(OEP)Th(OH)_2]_3^-$ to $[(OEP)Th(OH)_2]_3^{2-}$ in solution. The band at 799 nm shows a similar doubling in molar absorptivity from 1.9×10^4 to 3.7×10^4 M^{-1} cm^{-1} during the one-electron reduction of $[(OEP)Th(OH)_2]_3^-$. These spectral data are consistent with the stepwise formation of a π anion radical located first on one and then on two of the three porphyrin units of trimeric $[(OEP)Th(OH)_2]_3$. The addition of a third electron to $[(OEP)Th(OH)_2]_3$ leads to a dissociation of the trimer unit.

(13) Kadish, K. M. *Prog. Inorg. Chem.* **1986**, *34*, 435.

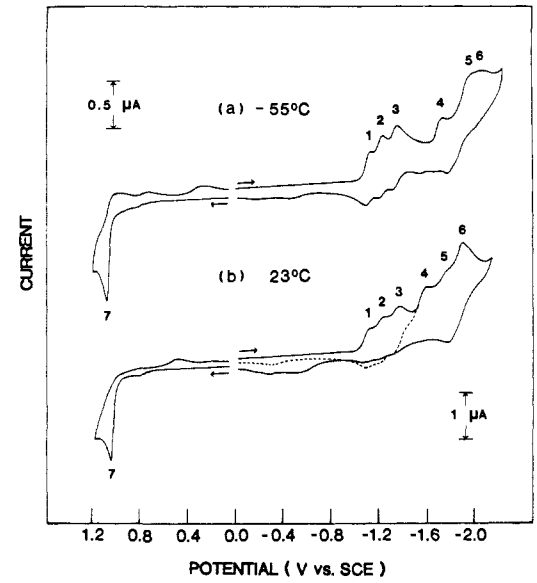

Figure 9. Cyclic voltammograms (scan rate 0.10 V/s) of 1.3×10^{-3} M $[(TPP)Th(OH)_2]_3$ in THF, 0.2 M TBAP, (a) at −55 °C and (b) at 23 °C.

Reduction of $[(TPP)Th(OH)_2]_3$. A cyclic voltammogram of $[(TPP)Th(OH)_2]_3$ in THF at −55 °C is shown in Figure 9a. Three reversible, one-electron-reduction processes occur between 0.00 and −1.50 V and are labeled as processes 1–3. The potentials for these three reductions occur at $E_{1/2} = -1.13$, −1.27, and −1.36 V and are shifted by 360–510 mV relative to processes 1–3 for the reduction of $[(OEP)Th(OH)_2]_3$ at −72 °C (see Table VIII).

Three additional irreversible reductions of $[(TPP)Th(OH)_2]_3$ are observed when the potential is scanned to −2.20 V. These occur at $E_p = -1.76$, −2.00, and −2.10 V in THF solutions at −55 °C and are labeled as peaks 4–6 in Figure 9a. These reactions were not spectrally characterized but most likely correspond to the formation of dianions localized on each of the three porphyrin units of $[(TPP)Th(OH)_2]_3$. Peaks 5 and 6 are overlapped in potential at −55 °C, but this is not the case at room temperature where all three peaks are separated in potential.

Figure 9b shows the room-temperature cyclic voltammogram of $[(TPP)Th(OH)_2]_3$ in THF at a scan rate of 0.10 V/s. The first three reductions (peaks 1–3) are reversible at this temperature if the cathodic scan is terminated at −1.50 V (see dashed line in Figure 9b). However, a new peak is observed at $E_p = -0.32$ V after scanning past the third reduction process and indicates that some decomposition of $[(TPP)Th(OH)_2]_3$ has occurred.

No return oxidations are coupled to processes 1–3 after scanning to −2.20 V at room temperature, and under these conditions, the reoxidation process at $E_p = -0.32$ V becomes much larger. A new oxidation at $E_p = -0.50$ V is also found under these experimental conditions and is assigned to oxidation of a product generated in a chemical reaction involving electroreduced $[(TPP)Th(OH)_2]_3$.

Spectroelectrochemical data indicate that the initial three reductions of $[(TPP)Th(OH)_2]_3$ occur at porphyrin ring based orbitals. The original trimeric species has a UV–visible absorption spectrum characterized by a Soret band at 414 nm and two visible bands at 552 and 587 nm in THF, 0.2 M TBAP. Figure 7b illustrates the ESR spectrum of singly reduced $[(TPP)Th(OH)_2]_3^-$. The spectrum centered at $g = 2.002$ resembles that of $[(OEP)Th(OH)_2]_3^-$ and is clearly that of a porphyrin π anion radical. Figure 10 illustrates the changes that occur in the UV–visible spectrum of $[(TPP)Th(OH)_2]_3$ when the potential is sequentially scanned from 0.00 to −1.24 V, −1.24 to −1.34 V, and −1.34 to −1.54 V in THF, 0.2 M TBAP. The final spectrum obtained after the

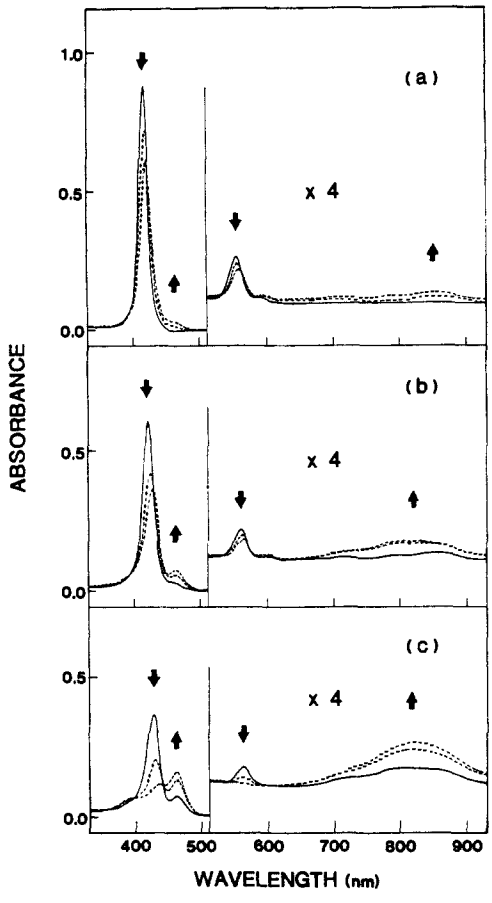

Figure 10. UV–visible spectra of $[(TPP)Th(OH)_2]_3$ in THF, 0.2 M TBAP, upon scanning (a) from 0.00 to −1.24 V; (b) from −1.24 to −1.34 V; and (c) from −1.34 to −1.54 V at a scan rate of 1 mV/s.

addition of three electrons to the neutral complex has absorption bands at 434, 460, and 815 nm and is characteristic of a porphyrin π anion radical.[13] Partial dissociation of the trimer may occur during controlled-potential electrolysis, but the voltammetric data are consistent with the stepwise formation of $[(TPP)Th(OH)_2]_3^-$, $[(TPP)Th(OH)_2]_3^{2-}$, and $[(TPP)Th(OH)_2]_3^{3-}$ where one electron has been added sequentially to each of the three porphyrin π ring systems.

Oxidation of $[(OEP)Th(OH)_2]_3$. Figure 6a shows a cyclic voltammogram of $[(OEP)Th(OH)_2]_3$ in THF at −72 °C. The first oxidation is a reversible three-electron-transfer process, which occurs at $E_{1/2}$ = 0.66 V. Three additional reversible oxidations are also observed at this temperature and are labeled as peaks 8–10 in Figure 6a. These oxidations occur at $E_{1/2}$ = 0.99, 1.04, and 1.14 V. Some decomposition of oxidized $[(OEP)Th(OH)_2]_3$ is also observed when the potential is scanned to 1.46 V. This is evidenced by the presence of rereduction peaks at E_p = 0.74 V (peak 11) and 0.88 V (peak 12).

The room-temperature cyclic voltammogram of $[(OEP)Th(OH)_2]_3$ in THF is shown in Figure 6b, and a rotating-disk voltammogram of the same solution is shown in Figure 6c. The cyclic voltammogram indicates that process 7 is a reversible diffusion-controlled three-electron oxidation, which, at room temperature, occurs at $E_{1/2}$ = 0.69 V. The measured $|E_{pa} - E_{pc}|$ = 20 mV, $|E_p - E_{p/2}|$ = 20 mV, and constant $i_p/v^{1/2}$ are consistent with a diffusion-controlled three-electron-transfer process. The ratio of anodic to cathodic current is also consistent with a reversible diffusion-controlled reaction. If the potential scan is reversed immediately after peak 7, then $i_{pa} = i_{pc}$.

Rotating-disk experiments further demonstrate the three-electron nature of this oxidation. The current for process 7 is 3 times larger than the reduction current for process 1 or 2 in Figure 6c. However, the ratio of current for process 7 to process 1 is less than the theoretical value of 5.2 for a simultaneous three-electron transfer by cyclic voltammetry and varies between 2.9

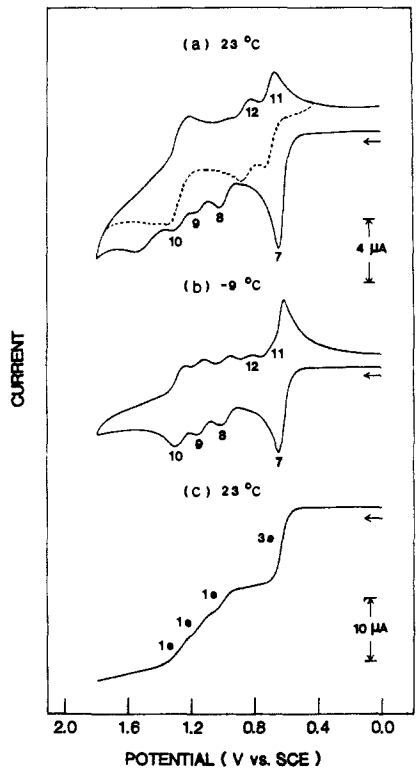

Figure 11. Cyclic voltammograms of 1.1×10^{-3} M $[(OEP)Th(OH)_2]_3$ in PhCN, 0.2 M TBAP, (a) at 23 °C (scan rate 0.10 V/s) and (b) at −9 °C (scan rate 0.10 V/s) and (c) rotating-disk voltammogram of the same complex at 23 °C. Rotation rate 1600 rpm.

and 3.1 in PhCN or CH_2Cl_2. A larger value of 3.8 ± 0.3 is obtained in THF. The theoretical current for oxidation or reduction of a given complex by cyclic voltammetry is proportional to $n^{3/2}$ where n is the number of electrons transferred in a single-electron-transfer step.[14] Thus, the overall electron-transfer process in peak 7 is attributed to three overlapping single-electron transfers where each one-electron oxidation becomes progressively easier (an electrochemical EEE type mechanism).[15]

The peaks 8 and 9 are not well-defined at room temperature due to their proximity to the solvent discharge limit. However, there is an overlapping broad peak located at E_p = 1.10 V. There is no return reduction peak for process 7 if the potential is scanned to 1.20 V, and under these conditions, there are also two additional reversible reductions, which occur at $E_{1/2}$ = 0.80 V (wave 11) and 0.96 V (wave 12). These latter two processes remain upon multiple-oxidative scans and are apparently related to decomposition products from $[(OEP)Th(OH)_2]_3$.

Similar room-temperature electrochemical behavior of $[(OEP)Th(OH)_2]_3$ is observed in THF and PhCN. This is illustrated by the voltammogram in PhCN (Figure 11a), which is quite similar to the one obtained in THF at room temperature (Figure 6b). However, the voltammograms are better defined in PhCN at lower temperatures, and the fact that three one-electron-transfer processes follow the initial overall three-electron oxidation is very clearly demonstrated in PhCN at −9 °C (Figure 11b). The results of cyclic voltammetry of $[(OEP)Th(OH)_2]_3$ at low temperature are consistent with results obtained for the same solution at room temperature by rotating-disk voltammetry (Figure 11c) and clearly illustrate that the current for the initial oxidation of $[(OEP)Th(OH)_2]_3$ is 3 times higher than current for each of the three following one-electron oxidations.

The initial oxidation of $[(OEP)Th(OH)_2]_3$ is assigned as abstraction of an electron from each of the three porphyrin π ring systems. This is based on spectroelectrochemical data and on the $\Delta E_{1/2}$ of 2.20 V between the first ring-centered reduction and the

(14) Bard, A. J.; Faulkner, L. R. *Electrochemical Methods*; Wiley: New York, 1980; p 218.
(15) Polcyn, D. S.; Shain, I. *Anal. Chem.* **1966**, *38*, 370.

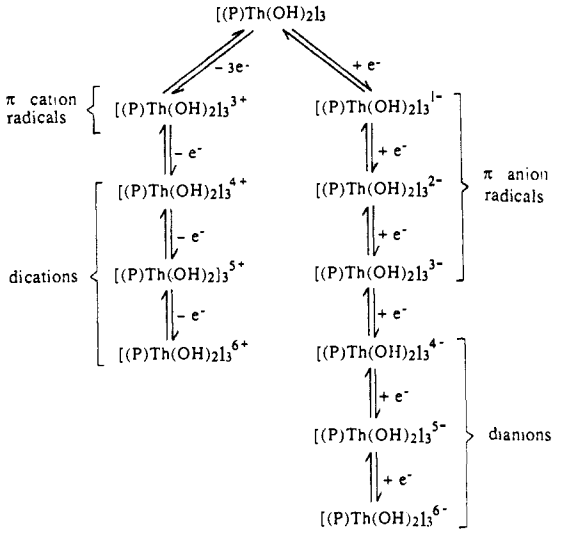

Figure 12. Overall scheme for oxidation and reduction of trimeric $[(P)Th(OH)_2]_3$.

first oxidation of the complex in THF.[16] An oxidation of Th(IV) or a reversible OH^- oxidation[17] is not likely to occur in this overall three-electron-transfer step.

Oxidation of $[(TPP)Th(OH)_2]_3$. A low-temperature cyclic voltammogram of $[(TPP)Th(OH)_2]_3$ is shown in Figure 9a. The first oxidation (peak 7) involves an irreversible, three-electron-transfer process at E_p = 1.08 V, but there is only a small rereduction peak associated with this process. The room-temperature cyclic voltammogram (Figure 9b) is similar to the voltammogram at low temperature. A small rereduction peak is located at E_p = 0.48 V and is associated with a product of the chemical reaction following the initial three-electron oxidation. The site of oxidation in $[(TPP)Th(OH)_2]_3$ is also postulated to occur at the porphyrin π ring system.

Summary. This study has provided the first characterization of a trimeric metalloporphyrin containing three discrete metalloporphyrin units. The formation of trimeric $[(P)Th(OH)_2]_3$ is demonstrated to occur both in the solid state and in solution. A dissociation of the trimer occurs at porphyrin concentrations of 10^{-5}–10^{-7} M, but, at the more concentrated (polarographic) concentrations of 10^{-3} M, all of the compound is in the associated form.

The best stability is observed for $[(OEP)Th(OH)_2]_3$, which can be oxidized in a single three-electron-transfer step to give $[(OEP)Th(OH)_2]_3^{3+}$ or reduced in three one-electron-transfer steps to successively give $[(OEP)Th(OH)_2]_3^-$, $[(OEP)Th(OH)_2]_3^{-2}$, and $[(OEP)Th(OH)_2]_3^{-3}$. The potentials for these three one-electron additions are separated by 170–210 mV in THF at −72 °C. Smaller separations of 110–140 mV are observed for reduction of $[(TPP)Th(OH)_2]_3$ in THF at −55 °C, but, for this complex, the formation of a stable trimer containing one, two, or three porphyrin dianion units is possible as shown in Figure 12.

The potential separation between formation of the π anion radical $[(TPP)Th(OH)_2]_3^{3-}$ and formation of $[(TPP)Th(OH)_2]_3^{4-}$, which contains one porphyrin dianion unit and two porphyrin anion radical units, is 400 mV. This value agrees perfectly with separations between π anion radicals and dianions of numerous other monomeric tetraphenylporphyrins.[13,16]

The formation of a π porphyrin cation radical occurs reversibly in a single simultaneous step involving all three porphyrin units of $[(P)Th(OH)_2]_3$. This is shown by the values of $|E_{pa} - E_{pc}|$ and $|E_p - E_{p/2}|$ = 20 mV and compares to the theoretical 60 mV separation expected for three one-electron reductions of a trimer containing three identical noninteracting electroactive sites.[18] In contrast to the initial oxidation, the abstraction of three additional electrons from $[(OEP)Th(OH)_2]_3^{3+}$ occurs via single one-electron-transfer abstractions to give $[(OEP)Th(OH)_2]_3^{4+}$, $[(OEP)Th(OH)_2]_3^{5+}$, and $[(OEP)Th(OH)_2]_3^{6+}$. The potential separation between formation of the three isolated π cation radicals on $[(OEP)Th(OH)_2]_3^{3+}$ and the single dication on $[(OEP)Th(OH)_2]_3^{4+}$ is 330 mV in THF at −72 °C. This agrees with similar separations between π cation radicals and dications of numerous monomeric octaethylporphyrins[16] and thus implies that abstraction of a single electron from one of the three equivalent porphyrin units of $[(OEP)Th(OH)_2]_3^{3+}$ has a similar energy barrier as abstraction of one electron from the porphyrin π cation radical of a monomeric complex. However, after formation of $[(OEP)Th(OH)_2]_3^{+4}$, an interaction of the porphyrin units occurs and the additional positive charge is distributed onto the other porphyrin units, thus resulting in an increased energy barrier for the following oxidations, which are separated by 50–100 mV in THF at −72 °C.

Acknowledgment. Support of the National Science Foundation (Grants No. CHE-8515411 and INT-8413696) and the CNRS is gratefully acknowledged.

Registry No. $[(TPP)Th(OH)_2]_3 \cdot 2H_2O \cdot 3C_7H_{16}$, 115321-85-2; (TPP)$ThCl_2$, 115321-86-3; $[(OEP)Th(OH)_2]_3$, 115321-87-4; (OEP)$ThCl_2$, 115321-88-5; $[(OEP)Th(OH)_2]_3^-$, 115559-81-4; $[(OEP)Th(OH)_2]_3^{2-}$, 115559-80-3; $[(OEP)Th(OH)_2]_3^{3-}$, 115559-79-0; $[(OEP)Th(OH)_2]_3^{3+}$, 115481-57-7; $[(OEP)Th(OH)_2]_3^{4+}$, 115559-82-5; $[(OEP)Th(OH)_2]_3^{5+}$, 115559-83-6; $[(OEP)Th(OH)_2]_3^{6+}$, 115481-58-8; $[(TPP)Th(OH)_2]_3^-$, 115511-89-2; $[(TPP)Th(OH)_2]_3^{2-}$, 115511-88-1; $[(TPP)Th(OH)_2]_3^{3-}$, 115481-56-6.

Supplementary Material Available: Tables of hydrogen atom fractional coordinates, anisotropic temperature factors, and torsion angles for $[(TPP)Th(OH)_2]_3 \cdot 2H_2O$ (3 pages); table of observed and calculated structure factors (4 pages). Ordering information is given on any current masthead page.

(16) Felton, R. H.; Linschitz, H. *J. Am. Chem. Soc.* **1966**, *88*, 1113.
(17) Tsang, P. K. S.; Cofre, P.; Sawyer, D. T. *Inorg. Chem.* **1987**, *26*, 3604.
(18) Flanagan, J. B.; Margel, S.; Bard, A. J.; Anson, F. C. *J. Am. Chem. Soc.* **1978**, *100*, 4248.
(19) Walker, N.; Stuart, D. *Acta Crystallogr., Sect. A: Found. Crystallogr.* **1983**, *A39*, 158–166.
(20) *International Tables for X-ray Crystallography*; Kynoch: Birmingham, England, 1974; Vol. IV, Tables 2-2B and 2-3-1.